DR. CAROLINA VOIGT (Orcid ID : 0000-0001-8589-1428)

MS. CLAIRE C TREAT (Orcid ID : 0000-0002-1225-8178)

Article type : Primary Research Articles

Ecosystem carbon response of an Arctic peatland to simulated permafrost thaw

Running head: Carbon fluxes of thawing permafrost peatlands

Carolina Voigt^{1,2*}, Maija E. Marushchak^{2,3}, Mikhail Mastepanov^{4,5}, Richard E. Lamprecht², Torben R. Christensen^{4,5}, Maxim Dorodnikov⁶, Marcin Jackowicz-Korczyński^{4,5}, Amelie Lindgren^{5,7}, Annalea Lohila⁸, Hannu Nykänen², Markku Oinonen⁹, Timo Oksanen², Vesa Palonen¹⁰, Claire C. Treat², Pertti J. Martikainen², Christina Biasi²

¹Department of Geography, University of Montréal, QC H2V 2B8 Montréal, Canada

² Department of Environmental and Biological Sciences, University of Eastern Finland, 70211 Kuopio, Finland

³ Department of Biological and Environmental Science, University of Jyväskylä, 40014 Jyväskylä, Finland

⁴ Department of Bioscience, Arctic Research Centre, Aarhus University, 4000 Roskilde, Denmark

This article has been accepted for publication and undergone full peer review but has not been through the copyediting, typesetting, pagination and proofreading process, which may lead to differences between this version and the Version of Record. Please cite this article as doi: 10.1111/gcb.14574

⁵ Department of Physical Geography and Ecosystem Science, Lund University, 22362 Lund, Sweden

⁶ Department of Soil Science of Temperate Ecosystems, Georg-August-University, 37073 Göttingen, Germany

⁷ Department of Physical Geography, Stockholm University, 10691 Stockholm, Sweden

⁸ Finnish Meteorological Institute, 00101 Helsinki, Finland

⁹ Finnish Museum of Natural History, University of Helsinki, 00014 Helsinki, Finland

¹⁰ Department of Physics, University of Helsinki, 00014 Helsinki, Finland

corresponding author. Email: carolina.voigt@umontreal.ca, Phone.: +1 438 345 9045

Keywords: Greenhouse gas, climate warming, permafrost-carbon-feedback, CO₂, methane oxidation, mesocosm

ABSTRACT

Permafrost peatlands are biogeochemical hot spots in the Arctic as they store vast amounts of carbon. Permafrost thaw could release part of these long-term immobile carbon stocks as the greenhouse gases (GHGs) carbon dioxide (CO₂) and methane (CH₄) to the atmosphere, but how much, at which time-span and as which gaseous carbon species is still highly uncertain. Here we assess the effect of permafrost thaw on GHG dynamics under different moisture and vegetation scenarios in a permafrost peatland. A novel experimental approach using intact plant–soil systems (mesocosms) allowed us to simulate permafrost thaw under near-natural conditions. We monitored GHG flux dynamics via high-resolution flow-through gas measurements, combined with detailed This article is protected by copyright. All rights reserved.

monitoring of soil GHG concentration dynamics, yielding insights into GHG production and consumption potential of individual soil layers. Thawing the upper 10–15cm of permafrost under dry conditions increased CO_2 emissions to the atmosphere (without vegetation: 0.74±0.49 vs. 0.84±0.60g CO_2 –C m⁻²d⁻¹; with vegetation: 1.20±0.50 vs. 1.32±0.60g CO_2 –C m⁻²d⁻¹, mean±SD, pre- and post-thaw, respectively). Radiocarbon dating (¹⁴C) of respired CO_2 , supported by an independent curve fitting approach, showed a clear contribution (9–27%) of old carbon to this enhanced post-thaw CO_2 flux. Elevated concentrations of CO_2 , CH_4 , and dissolved organic carbon at depth indicated not just pulse emissions during the thawing process, but sustained decomposition and GHG production from thawed permafrost. Oxidation of CH_4 in the peat column, however, prevented CH_4 release to the atmosphere. Importantly, we show here that, under dry conditions, peatlands strengthen the permafrost–carbon feedback by adding to the atmospheric CO_2 burden post-thaw. However, as long as the water table remains low, our results reveal a strong CH₄ sink capacity in these types of Arctic ecosystems pre- and post-thaw, with the potential to compensate part of the permafrost CO_2 losses over longer timescales.

1. INTRODUCTION

Permafrost soils are large carbon (C) reservoirs, storing ~1035Pg (=1035 billion tons) of organic C in the upper 3m (Hugelius *et al.*, 2014). These vast C stocks have accumulated over thousands of years in the form of frozen and seasonally thawed soil, litter and peat (Koven *et al.*, 2011). Thawing of permafrost as a result of climate warming exposes these long-term immobile belowground C stocks to microbial decomposition and remobilization, leading to the release of the greenhouse gases (GHGs) carbon dioxide (CO₂) and methane (CH₄) to the atmosphere (Hayes *et al.*, 2014). As enhanced vegetation productivity is expected to compensate little to none of this permafrost C release (Abbott *et al.*, 2016), the increased concentration of these gases within the atmosphere will further amplify warming (Dorrepaal *et al.*, 2009, Hobbie *et al.*, 2002, Schuur *et al.*, 2013). However, the magnitude of this permafrost–C feedback is poorly constrained (McGuire *et al.*, 2018) and not included in current IPCC projections, likely underestimating the climate feedback of the Arctic (Ciais *et al.*, 2013, Koven *et al.*, 2011, Schaefer *et al.*, 2014). Recent climate simulations predict an additional warming of ~0.2°C caused by permafrost C loss by the end of this century (Burke *et al.*, 2017, Schaefer *et al.*, 2014).

Permafrost is warming across the globe (Biskaborn et al., 2019) and within the last two decades upper permafrost temperatures have risen by 0.5-2.0°C (Romanovsky et al., 2010). Subarctic regions, where permafrost temperatures are already close to zero, are particularly vulnerable to near-term C losses with permafrost thaw (Koven et al., 2015). These areas, underlain by discontinuous and sporadic permafrost, currently experience extensive permafrost degradation (Sweden: Åkerman & Johansson, 2008, Norway: Borge et al., 2017, Canada: Helbig et al., 2017a, Alaska: Lara et al., 2016, Russia: Romanovsky et al., 2010). The Subarctic is also the region where highly sensitive, warm permafrost coincides with the occurrence of vast peatlands (Gorham, 1991). These organic soils, with their thick peat deposits, are biogeochemical hot spots in the Arctic, as they are by far the largest C reservoirs (Gorham, 1991, Hugelius et al., 2014, Tarnocai et al., 2009), storing ~296 Pg C (0–3m, land cover classes histosols and histels; Hugelius et al., 2014) – almost one third of the total organic C stored in the upper 3m of soils in the permafrost region. About half of these C stocks (147 Pg) occur in organic soils underlain by permafrost (histels; Hugelius et al., 2014). Due to their location in the rapidly warming southern Arctic, and their large ice content in the porous peat material, permafrost peatlands are vulnerable to thaw and thermokarst formation (Hugelius et al., 2012, Sannel & Kuhry, 2011), and degradation of permafrost peatlands is observed in the entire subarctic region (Baltzer et al., 2014, Borge et al., 2017, Helbig et al., 2017a, Malmer et al., 2005).

Thawing of permafrost (ground that remains continuously frozen for at least two consecutive years) can occur either gradually, seen as a deepening of the active layer (annually thawing soil layer above the permafrost), or more abruptly, when thawing of ice-rich permafrost creates collapse features

and thermokarst (Hugelius et al., 2011, Olefeldt et al., 2016, Schuur et al., 2008). Ground collapse severely alters site hydrology, leading to either drying or wetting depending on local drainage conditions. However, hydrological and landscape changes associated with permafrost thaw and associated changes in C release are difficult to predict, thereby posing a large uncertainty in predicting the future C balance in these regions. Currently, we lack sufficient understanding of the ratio of CO₂ vs. CH₄ of total gaseous C release, which will have important consequences for radiative forcing due to a \sim 30 times higher warming potential of CH₄ per mass unit (Knoblauch et al., 2018, Myhre et al., 2013, Schädel et al., 2016, Schuur et al., 2015). An increasing number of studies show that permafrost thaw promotes CO_2 and CH_4 production potential in soils (Hodgkins *et al.*, 2014, Schädel et al., 2016). Hence, the atmospheric C release from permafrost soils is anticipated to increase substantially as permafrost thaws (Koven et al., 2011, Koven et al., 2015, Schneider von Deimling et al., 2012, Schuur et al., 2009, Zhuang et al., 2006). While the largest C losses are expected to occur when thawing takes place under oxic conditions due to the proportionally larger production of CO₂ vs. CH₄ (Lee et al., 2012, Schädel et al., 2016, Schuur et al., 2015, Treat et al., 2014), recent long-term incubations predict an equally large permafrost-C feedback from anoxic soils, promoted by CH_4 production (Knoblauch *et al.*, 2018).

Despite growing evidence of enhanced gaseous C production in thawing permafrost soils, the effect of permafrost thaw on the ecosystem C balance remains poorly constrained, and field observations contradict model projections (Schädel *et al.*, 2018). Some key uncertainties of the permafrost-carbon feedback are related to 1) changes in vegetation cover and moisture conditions post-thaw, and 2) transformation of carbon in the soil profile. The major reasons for current uncertainties are of a practical nature: simulating the direct effect of permafrost thaw on biogeochemical cycling, without creating a mixed signal of thawing, soil warming, snow depth, moisture and vegetation changes (Mauritz *et al.*, 2017, Salmon *et al.*, 2016) is near to impossible under *in situ* conditions. Soil incubation studies, on the other hand, using homogenized soil samples or sub-cores taken out of context of the intact soil system, are valuable tools to assess the C decomposability and temperature This article is protected by copyright. All rights reserved. sensitivity of gaseous C production from thawed permafrost (Schädel *et al.*, 2016, Treat *et al.*, 2015). However, while soil incubation studies provide insight into soil processes and their environmental controls, they provide limited insights into the role of vegetation and the diverse transport and biogeochemical transformation processes along the soil profile. In many cases, gaseous C production at depth is decoupled from soil surface C emissions, especially in peatlands (Blodau & Moore, 2003a): even if CO₂ and CH₄ production rates in or near the permafrost are high, gases can be consumed (reduction of CO₂ to CH₄, oxidation of CH₄ to CO₂) while diffusing upwards through the soil profile (Dorodnikov *et al.*, 2013). Further, downward leaching of nutrients and dissolved C from the surface and soil rooting zone to deeper soil layers can be an important process supporting microbial activity at depth (Corbett *et al.*, 2013, Voigt *et al.*, 2017a, Wild *et al.*, 2016). All these processes determine whether permafrost thaw results in a net increase or decrease in ecosystem C emissions.

To directly assess how permafrost thaw affects the ecosystem GHG balance of permafrost peatlands, we developed an experimental set-up that allowed us to sequentially increase the thaw depth in intact plant–soil systems (mesocosms), with treatments simulating different vegetation and moisture scenarios. We used a specifically designed flow-through system combined with a laser instrument to obtain continuous measurements of CO₂ and CH₄, and complemented our flux observations with radiocarbon dating (14 C) of CO₂ fluxes and peat, as well as detailed auxiliary measurements: concentrations of CO₂, CH₄, dissolved organic C (DOC) and microbial biomass in the whole unfrozen part of the peat profile, as well as soil physical-chemical parameters. We hypothesize that thawing of permafrost will substantially alter the peatland C budget compared to pre-thaw conditions by increasing old C release. Specifically, we expect post-thaw release of CO₂ and CH₄ previously trapped in the permafrost layer, seen as short-term emissions peaks, but also a more sustained gaseous C production at depth via the enhanced substrate pool of freshly thawed permafrost. We further expect post-thaw C emissions to be regulated by moisture conditions in the peat profile, with wet conditions reducing CO₂ emissions but instead promoting CH₄ production and release.

2. MATERIAL AND METHODS

2.1 Study site

The intact plant-soil systems (mesocosms) used in this study were collected in a palsa mire ("Peera Palsa", 68.88°N, 21.05°E) in the discontinuous/sporadic permafrost zone of Finnish Lapland. Peat plateaus and palsas, permafrost peatlands uplifted above the surrounding mires by frost heave, are a common feature in the Subarctic (Borge *et al.*, 2017, Kuhry, 2008, Seppälä, 2006). As a result of permafrost uplift, the water table in these permafrost peatlands is low (Estop-Aragonés *et al.*, 2018a, Nykänen *et al.*, 2003, Turetsky *et al.*, 2002). The uplifted palsa surface is covered by typical palsa vegetation, dominated by *Empetrum nigrum* subsp. *hermaphroditum* and other dwarf shrubs such as *Vaccinium vitis-idaea* L., *Betula nana* L., and herbaceous plants, such as *Rubus chamaemorus* L., as well as lichens (mostly *Cladonia* spp.). Mosses (*Dicranum* spp., *Polytrichum* spp., *Pleurozium* spp, *Sphagnum spp.*) occur in the wetter parts of the palsa. The vegetated palsa surface is interspersed with patches of bare peat, naturally free of vascular plants, occurring regularly in uplifted permafrost peatlands (Marushchak *et al.*, 2011, Repo *et al.*, 2009, Seppälä, 2003, Seppälä, 2006). The site is described in greater detail in the Supporting Information.

2.2 Collection of mesocosms and experimental design

We collected 16 intact peat mesocosms ($\emptyset = 10$ cm, length ~80cm) from vegetated (8 mesocosms with typical, low-statured palsa vegetation) and naturally bare (8 mesocosms without vascular plants and only covered sporadically with lichens) parts of the palsa complex, using a custom-made steel corer (Fig. S1) (Voigt *et al.*, 2017b). Due to the comparatively small surface area, and to keep root damage during sampling to a minimum, larger vascular plants such as *Betula nana* L. were excluded from the mesocosms. However, the vegetation on the mesocosms (*Empetrum nigrum* subsp. *Hermaphroditum*, interspersed with *Vaccinium vitis-idaea* L, *Rubus chamaemorus* L., mosses and

lichens) was representative of the palsa surface (Fig. S1). The peat cores extended from the active layer (thickness ~65cm) down to the upper permafrost (thickness ~15cm). The cores were kept intact and were frozen immediately upon sampling. We used a freezer with custom-made temperature control to ensure storage in mild freezing temperatures (minimum temperature: -5°C), representing natural winter conditions beneath the snow cover. Prior to mesocosm collection we measured *in situ* flux rates of CO_2 and CH_4 from each sampling location at the study site, using the manual chamber technique (see Supporting Information for details).

After five months of storage, mimicking the winter period, the mesocosms were set up in a climatecontrolled chamber (BDR16 Reach-in plant growth chamber, CONVIRON, Winnipeg, Canada), allowing regulation of air temperature (adjusted to +10°C) and light levels (PAR at full light \leq 800 µmol m⁻² s⁻¹). The light levels were adjusted to represent a typical diurnal rhythm of the snow-free season in the region (18h full light, 4h of darkness, 1h of reduced light when transitioning from day to night and reverse).

We applied two distinct moisture treatments: while the water table in half of the mesocosms was kept at natural level (>50cm below surface, "dry"), we artificially raised the water table level in another subset of the cores to 5–10cm below surface ("wet"). The vegetation and moisture scenarios used in this study are referred to as DB (dry, bare), DV (dry, vegetated), WB (wet, bare), and WV (wet, vegetated). Step-wise thawing was achieved by placing the mesocosms in a saltwater-filled and glycol-circulated bath at temperatures below 0°C, as described earlier (Voigt *et al.*, 2017b). In short, we sequentially unfroze the mesocosms from top to bottom in 5–20cm increments during six thawing stages, each lasting four weeks (Table S1). After unfreezing the full peat profile, measurements continued for three months, resulting in a total duration of the experiment of 32 weeks.

2.3 Flow-through system for carbon dioxide and methane fluxes

For gas flux measurements, the mesocosms were permanently covered with transparent (allowing photosynthesis to take place) plexiglas chambers (OD = 121.2mm, ID = 120mm, h = 250mm, V = 2.8L) connected to an air in- and outflow via two three-way-valves (STERITEX® 3W, CODAN Medical, Lensahn, Germany). We continuously measured fluxes of CO_2 (Net ecosystem exchange, NEE) and CH₄ by means of a flow-through system (Fig. S1, Fig. S2). This kind of flow-through system has been successfully used with up to nine monoliths (Mastepanov & Christensen, 2009), but - to our knowledge – never with this number of replicates of large, intact mesocosms including permafrost. Gas fluxes were calculated using the difference between the gas concentration in each individual chamber (i.e. of each mesocosm) and a reference line with ambient (i.e. atmospheric) gas concentration (=16+1 mesocosms). For this purpose, we installed a reference core, which was filled with sterilized sand. A pump with flow control (flow rate ~4L/min), connected to an overflow exhaust, provided stable inflow of ambient, outdoor air to each of the mesocosms and to the reference line. To reduce evapotranspiratory losses from the mesocosms, the inflow air was humidified before reaching the mesocosm headspace. To minimize pressure perturbations inside the chambers, the outflow was kept steady by seventeen downstream pumps, equipped with water traps, pumping air from the individual mesocosms with a stable flow rate of 200 mL min⁻¹ to a valve system (Fig. S1). The valve system (consisting of 16+1 valves) automatically switched the gas flow between the mesocosms every five minutes, directing the flow to an infrared laser for highresolution CO₂ and CH₄ concentration measurements (DLT-100, Los Gatos Research (LGR), CA, USA). Ten weeks into the experiment the gas analyzer was swapped with another laser instrument (G-2301, Picarro, CA, USA), since the former was required for a field experiment. However, during the swap both analyzers were running simultaneously for three days, in order to eliminate possible artefacts of using different gas analyzers on measured flux rates. Concentrations measured with the LGR were adjusted to fit the Picarro factory calibration.

Net C fluxes were derived from the difference in gas concentration between the chamber headspace of the mesocosm (outgoing air) and the reference line (incoming air) (Mastepanov & Christensen, 2009), and calculated as follows:

$$T = \frac{\Delta c \times f \times M \times p \times 60 \times 24}{R \times T \times A \times 10^6},$$

(1)

where F is the net flux [mg m⁻² d⁻¹; positive for fluxes directed towards the atmosphere], Δc the difference in gas concentration [ppm], f the flow rate [L min⁻¹], M the molar mass of the gas [g mol⁻¹], p the atmospheric pressure [Pa], R the ideal gas constant [8.314 J K⁻¹mol⁻¹], T the temperature in the chamber headspace [K], and A the core surface area [m²].

2.4 Carbon dioxide and methane along the soil profile

To determine the concentration of gases along the soil profile, we installed five custom-made soil gas collectors horizontally in each core at depths 5cm, 20cm, and 40cm below the surface, 10cm above the measured thaw depth, as well as 5cm below the measured thaw depth. The soil gas collectors consisted of a perforated nylon/polyamide tube (ID = 4mm, OD = 6mm, length = 10cm) wrapped in fine nylon net and connected to another nylon tube (ID = 2mm, OD = 4mm, length ~50cm) capped with a three-way-valve (STERITEX[®] 3W, CODAN Medical, Lensahn, Germany).

Soil gas sampling and analysis are described in detail by Voigt et al. (2017a, 2017b). Briefly, soil gas sampling followed two different methods, depending on whether the sample was taken below or above the water table level. When samples were taken below the water table level, the gas concentrations were analyzed from a 28mL dinitrogen (N₂) headspace after equilibration with a 7mL water sample. When samples were taken above the water table level, 15mL of sample were withdrawn from the gas collector. In both cases samples were transferred to pre-evacuated 12mL screw-cap vials (Labco Exetainer[®], Labco, UK). For samples taken below the water table level we This article is protected by copyright. All rights reserved.

used 25mL of the headspace gas, while for samples taken above the water table level we used the 15mL of sampled gas and diluted with 10mL of N_2 in the exetainers. All gas samples were analyzed via gas chromatography (Agilent 6890N, Agilent Technologies, Santa Clara, CA, USA), equipped with a flame ionization detector (FID) for CH₄ (Voigt *et al.*, 2017a). Carbon dioxide was analyzed using an infrared gas analyzer (Uras26 continuous gas analyzer, AO2000 series, ABB Analytical Systems, Zurich, Switzerland), requiring a small (1mL) sample volume. For both gas analyzers, samples with high concentration were diluted with N₂ to fit the standard range (Voigt *et al.*, 2017a).

To determine the amount of gas dissolved in pore water from the gas concentration in the equilibrated headspace, we calculated the temperature dependent solubility k_H of the individual gases based on Henry's law, with coefficients taken from Lide and Frederikse (1995):

$$k_{H} = k_{H}^{\theta} \times \exp\left(\frac{-\Delta_{soln}H}{R} \times \left(\frac{1}{T} - \frac{1}{T^{\theta}}\right)\right),$$
(2)

where k_H^{θ} is the Henry's law constant at standard temperature [CO₂: 0.0350 mol atm⁻¹, CH₄: 0.0014 mol atm⁻¹], $\frac{-\Delta_{soln}H}{R}$ the temperature coefficient [CO₂: 2400 K, CH₄: 1600 K], *T* the soil temperature at the depth where the sample was taken and T^{ϑ} the standard temperature [298.15 K]. See Supporting Information for details.

2.5 Dissolved organic carbon in soil pore water

We used Rhizon pore water samplers (Rhizosphere, Wageningen, The Netherlands) for nondestructive weekly to biweekly soil water sampling to cover the temporal variation of DOC. Water samplers were installed in three depths in each mesocosm: 5–10cm and 35–40cm below the soil surface (in the active layer) and 0–5cm below the maximum seasonal thaw depth (~65–70cm below the soil surface). Pre-evacuated 12mL screw-cap vials (Labco Exetainer[®], Labco, UK) connected to the Rhizon tubes were used to sample pore water (Voigt *et al.*, 2017b). Pore water samples were frozen until further analysis and amounts of DOC in the pore water were determined as described by Voigt *et al.* (2017a).

2.6 Soil analyses

Basic soil properties (soil organic matter content (SOM), total C and nitrogen (N) content as well as C to N ratio, bulk density, water-filled pore space (WFPS) and pH) were determined at the end of the experiment at 5–6 depths of each peat profile. Details on analyses of soil properties are given by Marushchak et al. (2011) and Voigt et al. (2017a, 2017b). Additionally, we determined the amounts of DOC, total dissolved N (TDN), and C and N stored in the microbial biomass using the chloroform fumigation extraction method: samples were fumigated in chloroform atmosphere for 24h, after which fumigated and non-fumigated samples were extracted using 0.5M K₂SO₄. Samples were analyzed with a TOC/TN analyzer (LiquicTOC II; Elementar, Hanau, Germany), and we corrected for incomplete extraction of microbial C (K_{EC} = 0.45) and N (K_{EN} = 0.54) (Brookes *et al.*, 1985, Vance *et al.*, 1987) for microbial biomass calculations.

2.7 Radiocarbon age of soil and respired carbon

To determine the age of respired C in the CO₂ flux before and after thawing we measured the ¹⁴C (radiocarbon) content of CO₂ by using the molecular sieve sampling technique (Biasi *et al.*, 2014, Palonen & Oinonen, 2013). To avoid obtaining a signal masked by the high background of recently fixed C by vegetation we limited the ¹⁴C analysis to the dry, bare mesocosms (DB, n = 4). High respiration derived from a recently fixed C pool would have otherwise interfered with the accurate detection of the changes in the soil ¹⁴C signal.

We took samples twice during the experiment: the first sample was taken in week 15 directly before thawing the permafrost, with the whole active layer of the mesocosms being unfrozen (thaw depth ~65cm). The second sample was taken in week 32 at the end of the experiment, after the full peat profile, including the upper ~15cm permafrost, had been unfrozen for 12 weeks. Using an adaptive sample preparation line (Palonen et al., 2013), the CO₂ samples were collected from surface emissions and analyzed for their radiocarbon ¹⁴C content at the AMS facility at the University of Helsinki, as described by Tikkanen et al. (2004). Briefly, CO₂ samples were collected from closed chambers by first scrubbing the chamber with CO2-free air to remove background CO2. Then, CO2 derived from surface emissions was passed through the molecular sieves until a minimum of 1mg of CO₂-C was collected. Additionally, subsamples of soil were dated from five layers along the peat profile of one of the replicates (DB 4). The ¹⁴C content of the respired CO₂, expressed as percent modern C (pMC), was corrected for mass-dependent fractionation using δ^{13} C values. We corrected the obtained pMC values for air contribution in the molecular sieves by using an isotope mixing model, as described by Biasi et al. (2014, 2011), assuming a δ^{13} C value of soil respiration of -26‰ as is typical for C_3 ecosystems, and using an atmospheric concentration of 103.1±0.2 pMC (mean±SE for March/April 2013, data from Hyytiälä Forestry Field Station (61°51' N, 24°17' E); M. Oinonen, personal communication). Ages were calculated as conventional radiocarbon ages (years before present (BP), AD 1950 = 0 years BP), applying a radiocarbon decay equation with -8033 as the mean lifetime of ¹⁴C (Stuiver & Polach, 1977).

2.8 Contribution of permafrost-derived carbon to the post-thaw carbon dioxide flux

To estimate the contribution of permafrost-derived CO_2 to post-thaw CO_2 fluxes during our experiment, we applied two independent approaches, based on 1) the radiocarbon age of the flux, and 2) curve-fitting of an exponential decay function.

2.8.1 Permafrost carbon contribution based on radiocarbon dates

To assess the contribution of permafrost-derived CO_2 to the overall CO_2 emissions after the full peat profile had been unfrozen, we used a two-pool isotope mixing model:

Permafrost CO₂ (%) =
$$\left(\frac{AP^{14}CO_2 - BP^{14}CO_2}{PF^{14}CO_2 - BP^{14}CO_2}\right) \times 100$$
, (3)

where $AP^{14}CO_2$ is the ¹⁴C content of CO_2 derived from the completely unfrozen core including 15cm of permafrost (week 32, 12 weeks after unfreezing the permafrost, n = 4), $BP^{14}CO_2$ is the ¹⁴C content of CO_2 emitted directly before thawing the permafrost (week 15, n = 3 due to too little amount of CO_2 captured in one of the molecular sieves), and $PF^{14}CO_2$ is the estimated age of CO_2 originating from the permafrost layer alone. Since the experimental set-up did not allow us to directly measure the ¹⁴C content of permafrost CO_2 , we estimated the ¹⁴C content of this permafrost-derived CO_2 based on the ¹⁴C content of the permafrost soil (Table S2; see Supporting Information for details).

2.8.2 Permafrost carbon contribution based on exponential decay function

To estimate the contribution of permafrost-derived CO_2 from all four treatments, while accounting for the higher decay rate of the more labile surface C pool (Schädel *et al.*, 2013), we fitted a 3parameter exponential decay function to measured daily CO_2 flux rates (normalized to g CO_2 -C kgC⁻¹ d⁻¹) from weeks 1–20. This time period included the complete thawing of the active layer (weeks 1– 16) as well as the active layer-permafrost interface (top 5cm of permafrost, weeks 17–20). We extended the exponential fits until the end of the experiment (week 32) and calculated the permafrost C contribution by comparing values measured during the permafrost thaw period (week 21 onwards) with values predicted by the exponential decay function. Periods of water table fluctuations in the wet mesocosms were excluded from the analysis (Table S3). Curve fitting was done in SigmaPlot version 13.0 and fits had to pass tests for normality and constant variance. For the calculation of cumulative C fluxes, flux rates, measured every ~90min per mesocosm, were interpolated linearly to obtain hourly flux rates. Cumulative sums of CO_2 and CH_4 fluxes were calculated for each thawing step (lasting 28 days), as well as for the whole duration of the experiment.

To comparatively assess the post-thaw release of all three important GHGs – CO₂, CH₄, and nitrous oxide (N₂O), we used previously published N₂O flux data from the same experiment (Voigt *et al.*, 2017b). Briefly, N₂O fluxes were measured 2–3 times per week via manual chamber sampling and subsequent analysis on a gas chromatograph (GC; Agilent 6890N, Agilent Technologies, Santa Clara, CA, USA). Cumulative sums of N₂O were derived by interpolating linearly between measurement points. To compare the radiative forcing strength of all three GHGs, we applied the commonly used Global Warming Potential (GWP) approach (Myhre *et al.*, 2013), and compared this approach with Sustained-flux Global Warming and Cooling Potentials (SGWP, SGCP) (Neubauer & Megonigal, 2015).

2.10 Statistical analyses

All statistical analyses were performed in R version 3.5.1. (R Core Team, 2018). Prior to statistical tests we assessed the distribution of data via visual inspection of histograms, density plots and Q-Q plots, in combination with the Shapiro-Wilk normality test. Statistical differences between CO₂ and CH₄ fluxes during thawing of the active layer vs. thawing of the permafrost layer were determined based on the four-week periods directly before thawing the permafrost (week 13–16) and after thawing the full permafrost (week 21–24). The lower active layer (thawed during weeks 13–16) and the permafrost layer both consisted of fen type peat material (Voigt *et al.*, 2017b), allowing for comparison of layers with similar peat quality. Due to the lower frequency of sampling, statistical differences for soil profile concentration of gases were calculated based on the full period of active

layer thawing (weeks 1–16) and thawing of the permafrost (weeks 17–32). We used Student's t-test for normally distributed variables and Welch's two-sample t-test when variables were not normally distributed. To test for differences between treatments in cumulative fluxes for each thawing step (CO_2 , CH_4 , N_2O , and the complete GHG budget), we applied a two-way ANOVA, coupled with Tukey's HSD post-hoc test. The ANOVA included surface type (bare/vegetated) and moisture (dry/wet) as explanatory variables (GHG ~ Type + Moisture). Periods of water table fluctuations in the wet mesocosm (water table level below 10cm) were excluded from the analysis when comparing mean pre- and post-thaw flux rates. However, emission peaks related to this temporary drying and rewetting of peat were included when assessing cumulative GHG budgets, to account for labile C losses.

3 RESULTS

3.1 Carbon dioxide fluxes

All treatments showed net CO₂ release to the atmosphere (Fig. 1a). Fluxes of CO₂ (NEE) ranged from -0.91 to 61.34g CO₂–C m⁻² d⁻¹, (Fig. S4–S7), averaging at 0.79±0.56 (DB), 1.41±0.81 (DV), 0.67±0.59 (WB), 1.02±0.98g CO₂–C m⁻² d⁻¹ (WV, mean±SD). Fluxes were higher when vegetation was present (Fig. 1a, Fig. 2, Table S3). While wet mesocosms displayed lower CO₂ fluxes than their dry counterparts (Fig. 2), the effect of moisture was not significant (Table S4). Importantly, although the surface layers initially displayed the highest overall CO₂ emission rates, these surface emissions declined as thawing of the active layer progressed, but we again observed a pronounced increase in CO₂ emissions, particularly in the dry mesocosms, during the later stage of the experiment, when thawing reached the permafrost layer (Fig. 2, Fig. 3, Table S3).

3.2 Methane fluxes

Methane fluxes over the whole duration of the experiment ranged from high uptake rates of -17.92mg CH₄–C m⁻² d⁻¹ to short-term emission peaks of 29.75mg CH₄–C m⁻² d⁻¹ (Fig. S4–S7), however, average fluxes showed CH₄ uptake over all treatments (DB: -2.17±1.63mg CH₄–C m⁻² d⁻¹, DV: -3.54±4.20mg CH₄–C m⁻² d⁻¹, WB: -0.32±0.51mg CH₄–C m⁻² d⁻¹, WV: -0.11±0.41mg CH₄–C m⁻² d⁻¹; mean±SD). The dry mesocosms (DB and DV) acted as clear sinks for CH₄, whereas the wet mesocosms were generally CH₄ neutral (Fig. 1b) but switched to CH₄ sinks after temporary drops in water table level (Fig. S3b). Thawing of permafrost did not increase CH₄ emissions, and had, in fact, a reverse effect: gradual deepening of the active layer, increasing the oxygenated soil volume, enhanced CH₄ uptake in the dry mesocosms, causing higher rates of CH₄ uptake post-thaw (Fig. 1b, Fig. 2, Table S3), and – except for one out of 16 mesocosms – permafrost thaw did not initiate CH₄ emissions. Methane uptake was largest in dry, vegetated mesocosms (DV), with maximum uptake rates of -11.9mg CH₄–C m⁻² d⁻¹ occurring post-thaw (mean: -3.8mg CH₄–C m⁻² d⁻¹; Table S3).

3.3 Temporal and spatial dynamics of carbon dioxide, methane, dissolved organic carbon and microbial biomass in the soil profile

The soil profile concentrations of gas and dissolved C were dynamic over time and with depth. Higher CO_2 concentrations occurred in deeper soil layers, particularly after thawing the permafrost, and the high concentrations lasted until the end of the experiment (Fig. 4a, Table S5). Carbon dioxide accumulated especially in the wet mesocosms (Fig. 4a). There, CO_2 concentrations peaked at values >60 000 ppm (ambient: ~390 ppm, Table S5), with the largest concentrations occurring in the deeper active layer, near the active layer–permafrost interface. Concentrations of CH_4 , on the other hand, were clearly elevated only in the lower part of the mesocosms, and especially in the This article is protected by copyright. All rights reserved. permafrost part (>300 ppm CH₄, Fig. 4b, Table S6). While some CH₄ peaks occurred in the peat profile directly after thawing, the mid- and upper active layer of all mesocosms (bare as well as wet) seemed to be zones of CH₄ consumption (Fig. 4b, Fig. S9–S11).

Concentrations of DOC displayed a similar trend as CO₂, with the largest DOC contents measured in the middle and lower layers of the peat profiles (Fig. 4c). Detailed soil analyses after complete thawing showed significantly larger amounts of DOC (and TDN) in the permafrost peat than in the active layer (Fig. S12, Table S9). Even though the largest amounts of microbial biomass C (and N) occurred in the surface soil (5cm below surface), microbial biomass C was larger in the permafrost compared to the lower active layer, especially in the wet mesocosms (Fig. S12).

3.4 Permafrost-derived carbon dioxide fluxes and age of respired carbon

Except for wet, vegetated mesocosms, the increase in CO_2 emissions post-thaw was significant across treatments compared to thawing of the active layer (weeks 21–24 vs. weeks 13–16, Fig. 2, Table S3). On average, post-thaw CO_2 fluxes were 15% higher (mean of all treatments, Table S3). When accounting for the different amounts of C exposed with each thaw stage (Fig. S13, S14), our curve fitting approach revealed a permafrost contribution (thawing of the upper 10–15cm of permafrost) to measured post-thaw CO_2 emissions of 22–31% (bare, DB) and 5–10% (vegetated, DV) when thawing occurs under dry conditions, and a small or no detectable permafrost contribution under wet conditions (Table 1, Fig. S15, Table S10)

Radiocarbon dating of soil and respired C of dry, bare mesocosms (DB) confirmed the permafrost contribution obtained via the curve fitting approach: a higher age of the post-thaw CO_2 flux of 1895±191yr BP (mean±SE) compared to the pre-thaw age (1542±158yr BP) (Fig. 3) suggests a maximum permafrost contribution of 23–27±5% (mean±SE, Table S10). Not accounting for the age

difference between bulk soil and respired C (Table S2) still resulted in a permafrost contribution of 16±4%.

3.5 Cumulative greenhouse gas budgets

Wet bare mesocosms displayed the lowest cumulative GHG emissions, expressed as global warming potential (GWP), on a 100yr time horizon (WB: 464g CO₂–eq m⁻², Fig. 5a). Dry conditions promoted GHG release (DB: 682g CO₂–eq m⁻²), and the highest emissions occurred in vegetated mesocosms (WV: 763g CO₂–eq m⁻², DV: 837g CO₂–eq m⁻²). The cumulative CH₄ fluxes were higher (*P*=0.050) under wet conditions, but neither the GHG balance (*P*=0.264) nor the CO₂ fluxes (*P*=0.351) differed significantly between moisture treatments (Table S4). In contrast, the vegetation cover played a role in regulating the cumulative CO₂ emissions, with significantly higher CO₂ emissions from vegetated mesocosms under both moisture regimes (*P*=0.045), affecting also the total GHG balance (*P*=0.081, Table S4).

4 DISCUSSION

The main goal of this study was to directly assess how permafrost thaw, simulated on intact mesocosms under near-field conditions, affects the atmospheric C balance of permafrost peatlands under various moisture and vegetation scenarios. We expected increased post-thaw CO₂ release under dry conditions, but enhanced CH₄ release if permafrost thaw results in a raised water table. Our results revealed a contribution of the exposed permafrost layer to post-thaw CO₂ fluxes under dry conditions (9–27%). Contrary to our expectations we did not observe enhanced CH₄ release from this type of peatland, despite elevated post-thaw CH₄ concentrations in the peat profile at depth. Instead, deeper active layers promoted the ecosystem's CH₄ sink function.

4.1 Gaseous carbon production and release from permafrost in post-thaw peatlands

We observed a detectable signal of permafrost C release from dry mesocosms, seen as sustained GHG production and increased CO₂ emissions post-thaw (Fig. 3, Fig. S15, Table S10). Due to the presence of more recalcitrant material at depth, surface soil generally accounts for the largest proportion of CO₂ production (Hicks Pries *et al.*, 2015, Walz *et al.*, 2017, Wang & Roulet, 2017), and CO₂ production rates often show a depth-dependent decline (Christensen *et al.*, 1999, Estop-Aragonés *et al.*, 2018a, Treat *et al.*, 2014). Peatlands, however, display a high organic C availability (Treat *et al.*, 2016) and the deep peat layers, preserved in the permafrost for centuries, can be relatively labile and produce a considerable amount of GHGs (Treat *et al.*, 2014, Wang & Roulet, 2017), showing a long-lasting sensitivity to warming (Dorrepaal *et al.*, 2009).

The higher radiocarbon age of respired C after permafrost thaw (Fig. 3) suggests, that this increase in post-thaw emissions was due to the contribution of older C pools, originating from the permafrost layers. The temporal and spatial dynamics of gases, DOC (Fig. 4a–c) and microbial biomass C and N (Fig. S12) in the peat column support the conclusion of enhanced permafrost C release: in both scenarios, dry and wet, CO₂ accumulated to a greater extent after thawing the permafrost, and both, CO₂ and DOC concentrations at depth increased with time after thaw and were largest at the end of the experiment, three months after thawing the permafrost (Fig. 4a, Fig. 4c). Together, these results clearly suggest not only the release of gaseous C previously trapped in permafrost, but a sustained decomposition at depth post-thaw, and on-going CO₂ production from the thawed permafrost peat material.

Our two independent estimates of the permafrost contribution to post-thaw CO₂ fluxes (curvefitting: ~10% (vegetated), ~22% (bare), ¹⁴C: ~23% (bare), dry scenario) fall within the range of those few studies presenting quantified estimates of old C contribution to soil respiration (11–28%: Estop-Aragonés *et al.*, 2018a, 4–22% (burned and unburned peat plateau): Estop-Aragonés *et al.*, 2018b, 4–23%: Schuur *et al.*, 2009). Unlike previous studies, however, our experimental design allows us to

provide a first, tentative estimate of the magnitude of changing C cycling patterns from a thawing permafrost peatland, with and without vegetation cover, immediately upon thaw. By directly linking enhanced CO₂ emissions to permafrost thaw, our study attests for the contribution of permafrost-derived C not only to respiration, but to ecosystem-scale CO₂ emissions.

Although our study was laboratory based, our mesocosm approach simulating in situ conditions allows us to draw conclusions on the post-thaw C balance of permafrost peatlands: first of all, the peat stratigraphy of the sampling site (bog peat underlain by fen-type peat material; Voigt et al., 2017b) is representative for the majority (~80%) of uplifted permafrost peatlands in the Northern Hemisphere (Treat et al., 2016). Second, measured C flux rates agreed well with in situ C fluxes at the study site, as well as CO_2 and CH_4 fluxes measured across a range of Eurasian permafrost peatlands (Fig. 6). While the studied palsa and other permafrost peatlands likely show larger in situ C uptake than we observed here due to better plant performance under field conditions, the vegetation on the mesocosms was active throughout the experiment, and CO₂ fluxes were showing diurnal variation following the established light cycle (Fig. S16–S17). Additionally, permafrost peatlands and other Arctic ecosystems frequently show net C losses during summer, and increasingly so as soils continue to warm (Grogan & Chapin, 2000, Lund et al., 2012, Lundin et al., 2016, Nykänen et al., 2003, Oechel et al., 1993, Voigt et al., 2017a, Zamolodchikov et al., 2000). Hence, recent climate change has weakened the cooling effect northern peatlands have exerted on our climate for the past ~10000 years (Frolking & Roulet, 2007). Recent field observations report C losses and a weakened CO₂ sink strength from peatlands spanning the Pan-Arctic, including boreal peatland landscapes (Euskirchen et al., 2014, Helbig et al., 2017a, Jones et al., 2017, O'Donnell et al., 2012).

We provide evidence that thawing peatlands may strengthen the permafrost–C feedback of the Arctic, especially if thawing occurs under dry conditions, or if enhanced vegetation growth is not able to compensate for increased belowground CO₂ losses. Our results highlight the vulnerability of deep, previously frozen peat to decomposition. Climate models neglecting the permafrost–C

feedback, particularly from peatlands, are thus likely underestimating CO_2 emissions from Arctic ecosystems as it continues to warm (Burke *et al.*, 2017, Schaefer *et al.*, 2014).

4.2 Effects of moisture conditions on post-thaw carbon fluxes

Wet sites are generally growing season sinks for CO₂ and sources of CH₄, resulting in an overall net C sink across ecosystem types, such as wet parts of palsa mires (Christensen *et al.*, 2012), wet sedge and tussock tundra (Lafleur *et al.*, 2012), and wetlands in permafrost peatland landscapes in tundra (Heikkinen *et al.*, 2002) and boreal regions (Helbig *et al.*, 2017a). Soil oxic conditions are a key regulator of soil CO₂ production (Schädel *et al.*, 2016, Treat *et al.*, 2014, Walz *et al.*, 2017), and the position of the water table level therefore critically governs the rate and magnitude of C emissions from peatlands (Blodau & Moore, 2003b, Moore & Knowles, 1989, Nykänen *et al.*, 2003, Regina *et al.*, 1999). Yet, whether the Arctic will become wetter or drier in a future climate is highly uncertain (Schuur *et al.*, 2015), and the patchiness of the mosaic-like Arctic landscape makes it difficult to predict future, and even current landscape-level C balances (Schneider von Deimling *et al.*, 2012, Shaver *et al.*, 2007, Sturtevant & Oechel, 2013).

The majority of studies currently predict a larger permafrost C feedback when thawing occurs under oxic conditions (Schädel *et al.*, 2016, Schuur *et al.*, 2015), with old C release from dry peat soils, but no old C contribution to the surface CO_2 flux from wet, thermokarst-affected areas (Estop-Aragonés *et al.*, 2018a, Estop-Aragonés *et al.*, 2018b). Interestingly, even though our study finds the permafrost C contribution to post-thaw CO_2 fluxes under wet conditions minor (Table 1), the cumulative CO_2 emissions in our study were not significantly lower in the wet mesocosms (Fig. 5, Table S4). We attribute the similarity among moisture treatments to two reasons: first, the important contribution of the well oxygenated upper 0–10cm of the soil profile to total respiration. Second, the cumulative CO_2 fluxes in the wet mesocosms were partly determined by short-term

emission peaks, associated with a temporarily lowered water table during the thawing process (Fig. S3a) and associated changes in peat redox chemistry caused by these water table fluctuations. These emission peaks show a reoxygenation of electron acceptors (Knorr & Blodau, 2009), but also indicate the presence of a labile C pool and active microbial community, well adapted to anaerobic conditions, as has been shown earlier for old peat soils (Diakova et al., 2016). Hence, the timing and magnitude of CO_2 emissions from wet mesocosms was governed by the position of the water table which, when lowered, enabled rapid out-diffusion of CO₂. Water table fluctuations are a common phenomenon in northern peatlands (Komulainen et al., 1998, Tuittila et al., 1999). Thus, even though CO_2 emissions from thaw-affected peatlands might be small as long as the peat column stays well water saturated, our results show that seasonally or annually varying moisture conditions occurring post-thaw must clearly be considered when drawing conclusions on ecosystem-scale C emissions associated with permafrost thaw. Not only can labile C be released via on-site CO₂ emissions, but it can further be relocated to aquatic systems via leaching and runoff processes (Olefeldt & Roulet, 2012). Due to the tight coupling of the hydrological and the C cycle, and associated relocation of C emissions (Vonk & Gustafsson, 2013), predicting and quantifying postthaw C emissions under wet conditions poses an even larger challenge than estimating the permafrost-C feedback in comparatively dry settings.

Unexpectedly, despite evident CH₄ accumulation at depth after permafrost thaw (Fig. 4b), wet conditions did not cause net CH₄ release to the atmosphere. Incubation experiments have shown that previously well-aerated soils that are exposed to sudden anoxic conditions display long lagtimes in CH₄ production (Knoblauch *et al.*, 2018, Knoblauch *et al.*, 2013, Treat *et al.*, 2015), and even under field conditions thawed permafrost peat layers may contribute only little to surface CH₄ emissions (Cooper *et al.*, 2017). In comparably dry soils such as permafrost peatlands, where the soil microbial communities are well adapted to oxic conditions, methanogen populations are small, and only establish with time (McCalley *et al.*, 2014). Such well oxygenated sites display a high oxidation potential, and methanogenesis is additionally suppressed by drying and rewetting cycles (Knorr & This article is protected by copyright. All rights reserved. Blodau, 2009) and the presence of alternative electron acceptors like sulfate, nitrate and iron (Bridgham *et al.*, 2013, Neubauer *et al.*, 2005). We observed an accumulation of CH_4 only in the lower part of the peat profile (Fig 4b), consisting of fen-type peat material (Voigt *et al.*, 2017b), likely an active CH_4 source before permafrost uplift. These results show that, to predict future CH_4 release from permafrost, understanding permafrost aggradation history is highly important, as the site hydrologic conditions during permafrost aggradation determine the initial activity, presence, or absence of methanogens and methanotrophs upon thaw.

4.3 Short- and long-term peatland carbon response and post-thaw greenhouse gas balance

We observed comparatively high CO₂ emissions derived from the seasonally-thawing active layer (Fig. 1, Fig. 2). We attribute the initially high CO₂ fluxes to the presence of labile substrates in the undecomposed bog peat in the upper peat profile (Voigt *et al.*, 2017b), plant and root respiration, as well as fresh litter inputs from vegetation that stimulated microbial growth (Fig. S12) and thus heterotrophic respiration. The top 5cm of the vegetated peat profiles (both, dry and wet) exhibited the largest microbial biomass C (Fig. S12), indicating high microbial activity in the surface soil rooting zone. These surface emissions decreased over time (Fig. 3) with depletion of the labile surface C pool as litter and other recent plant inputs decomposed. The presence of vegetation, however, likely fueled microbial activity at depth, thus promoting decomposition of this more persistent C pool: we observed larger dissolved C and N pools at depth in vegetated mesocosms than in bare mesocosms (Fig. S12), indicating downward transport of C. Also, microbial biomass C and N pools in the peat profile were significantly larger when vegetation was present (C: *P* = 0.006, N: *P* = 0.003, Fig. S12, Table S9). The input of fresh, plant-derived organics can lead to a positive priming effect, actively driving the decomposition of old organic matter (Kuzyakov, 2010) and GHG production at depth (Corbett *et al.*, 2013, Voigt *et al.*, 2017a, Wild *et al.*, 2016, Wild *et al.*, 2014).

As our mesocosms approach indicates both C pools, young and old, are tightly linked. In field observations, with annual vegetation dynamics and rapid C turnover, the labile surface C pool may thus well dominate short-term, seasonal C emissions, thereby masking the permafrost-C feedback. But, even if small compared to seasonal vegetation C dynamics, permafrost thaw provides an additional, persistent C pool at depth, with the potential to affect the peatland C balance over long timescales. Depending on the thickness of the organic layer, a gradually increasing thaw depth (current rate in Northern Scandinavia: ~1cm yr⁻¹; Åkerman & Johansson, 2008), together with warming of soils, could fuel microbial decomposition at depth for centuries.

While our study demonstrates that permafrost thaw in Arctic peatlands will likely release an additional CO₂ burden to the atmosphere, the future GHG balance of thawing permafrost peatlands depends on moisture and vegetation changes, as well as on the dynamics of the other major greenhouse gases CH₄ and N₂O, both of which have a stronger potential to warm our climate than CO₂. Besides releasing CO₂, the dry mesocosms acted as sinks for CH₄, and as reported in our earlier study (Voigt *et al.*, 2017b), the bare mesocosms were a source for N₂O, and increasingly so with permafrost thaw. Commonly, the GWP approach (Myhre *et al.*, 2013) is used to compare the warming effect caused by different GHGs, projected to a 100yr time scale. However, the applicability of the GWP metrics to project long-term radiative forcing of peatlands is limited, as this approach assumes one-time pulse emissions (Neubauer & Megonigal, 2015) rather than sustained GHG production from steadily increasing permafrost C and N pools made accessible as thaw deepens. Additionally, the direction of gas transport has major implications for net radiative forcing, requiring different metrics when projecting GHG uptake and emissions (Neubauer & Megonigal, 2015).

Although the overall GHG budget of all four treatments was governed by CO_2 fluxes (Fig. 5), N_2O emissions from dry, bare mesocosms accounted for 14% of CO_2 emissions (GWP100; Fig. 5). The same approach places CH_4 uptake at 2–3% (bare vs. vegetated) of CO_2 emissions, and slightly higher (7–8%) when applying a shorter time span (20yr, Fig. S18). When considering the pronounced CH_4

sink capacity in dry mesocosms via the SGWP/SGCP approach (Neubauer & Megonigal, 2015), we show here that CH_4 uptake can compensate post-thaw ecosystem CO_2 emissions by 14%–19%, (20yr vs. 100yr time horizon), and up to 27% on a 500yr time scale (Fig. 5, Fig. S19).

Methane oxidation frequently occurs in ecosystems of the northern high latitudes (dry upland tundra: Bartlett & Harriss, 1993, Jørgensen *et al.*, 2015, Lau *et al.*, 2015, Christiansen *et al.*, 2015, D'Imperio *et al.*, 2017, Arctic peatlands: Flessa *et al.*, 2008, Malhotra & Roulet, 2015, upland forests: Olefeldt *et al.*, 2013). Methane fluxes are the balance between CH₄ production by methanogens under anoxic conditions, and CH₄ consumption under oxic conditions (Lai, 2009). Even though we observed enhanced CH₄ concentrations at depth after thaw (>300 ppm vs. ~1.9 ppm ambient concentration), a thick oxidative layer prevented CH₄ release to the atmosphere in both dry and wet mesocosms (Fig S8–S11). While CH₄ production may increase under long-term anoxic conditions and inflow of surrounding fen waters containing methanogens, our study emphasizes the need to consider transport and transformation pathways of CH₄ in the soil column when attempting to project the role of permafrost CH₄ release.

Current models predict increased CH₄ release from Arctic ecosystems as permafrost thaws, due to increased surface wetness (Anisimov, 2007, Deng *et al.*, 2014, Koven *et al.*, 2015, Wilson *et al.*, 2017), and field observation show increased CH₄ emissions from wet, thermokarst-affected sites (Christensen *et al.*, 2004, Helbig *et al.*, 2017b, Johnston *et al.*, 2014, Olefeldt *et al.*, 2013, Turetsky *et al.*, 2002). In contrast, our study emphasizes the important role CH₄ uptake may play in offsetting the permafrost-C feedback caused by CO₂ emissions, as long as conditions stay dry. This is an important finding, considering that, in fact, mounting evidence suggests that permafrost degradation will lead to a reduction in wetland extent (Avis *et al.*, 2011) by increasing runoff and drainage (Haynes *et al.*, 2018, Liljedahl *et al.*, 2016, Malmer *et al.*, 2005, Swindles *et al.*, 2015). Considering the vast Arctic landmasses, enhanced surface drying and deeper thaw is likely to increase the Arctic CH₄ sink, with potential repercussions on the global CH₄ budget. In light of the current overestimation of CH₄

emissions from northern wetlands (Saunois *et al.*, 2016), our study highlights the relevance of CH_4 uptake from well drained Arctic soils, such as uplifted permafrost peatlands, considering the potential of these dry surfaces to counterbalance wetland CH_4 emissions (D'Imperio *et al.*, 2017, Treat *et al.*, 2018). Overall, improving our understanding of local hydrological settings and vegetation dynamics will be key to predicting changes of the carbon cycle in a warming Arctic.

Acknowledgements

This work was funded by the Nordic Center of Excellence DEFROST. The authors gratefully acknowledge further funding from the European Union FP7-ENV project PAGE21 (contract no. 282700), JPI Climate project COUP (decision no. 291691), the Academy of Finland projects CryoN (decision no. 132045) and RFBR project NOCA (decision no. 314630), and UEF strategic funding FiWER. C.V. received personal funding from the University of Eastern Finland's doctoral program in Environmental Physics, Health, and Biology, and the Emil Aaltonen Foundation, as well as travel support from COST Action ABBA (ES0804), NordSIR, and NORDFLUX. We are grateful to Igor Marushchak, Hanne Säppi, Tatiana Trubnikova, and Kateřina Diáková for their help with practical work, and wish to thank Christina Schädel and Gabriel Hould Gosselin for valuable discussions, as well as three anonymous reviewers whose comments helped to greatly improve this manuscript.

- Abbott BW, Jones JB, Schuur EaG *et al.* (2016) Biomass offsets little or none of permafrost carbon release from soils, streams, and wildfire: an expert assessment. Environmental Research Letters, **11**, 034014.
- Åkerman HJ, Johansson M (2008) Thawing permafrost and thicker active layers in sub- arctic Sweden. Permafrost and Periglacial Processes, **19**, 279-292.
- Anisimov OA (2007) Potential feedback of thawing permafrost to the global climate system through methane emission. Environmental Research Letters, **2**, 045016.
- Avis CA, Weaver AJ, Meissner KJ (2011) Reduction in areal extent of high-latitude wetlands in response to permafrost thaw. Nature Geoscience, **4**, 444-448.
- Baltzer JL, Veness T, Chasmer LE, Sniderhan AE, Quinton WL (2014) Forests on thawing permafrost: fragmentation, edge effects, and net forest loss. Global Change Biology, 20, 824-834.
- Bartlett KB, Harriss RC (1993) Review and Assessment of Methane Emissions from Wetlands. Chemosphere, **26**, 261-320.
- Biasi C, Jokinen S, Marushchak ME, Hamalainen K, Trubnikova T, Oinonen M, Martikainen
 PJ (2014) Microbial Respiration in Arctic Upland and Peat Soils as a Source of Atmospheric Carbon Dioxide. Ecosystems, 17, 112-126.
- Biasi C, Tavi NM, Jokinen S *et al.* (2011) Differentiating sources of CO₂ from organic soil under bioenergy crop cultivation: A field-based approach using ¹⁴C. Soil Biology and Biochemistry, **43**, 2406-2409.
- Biskaborn BK, Smith SL, Noetzli J et al. (2019) Permafrost is warming at a global scale. Nature Communications, **10**, 264.

- Blodau C, Moore TR (2003a) Experimental response of peatland carbon dynamics to a water table fluctuation. Aquatic Sciences, 65, 47-62.
 Blodau C, Moore TR (2003b) Micro-scale CO₂ and CH₄ dynamics in a peat soil during a
 - Blodau C, Moore TR (2003b) Micro-scale CO_2 and CH_4 dynamics in a peat soil during a water fluctuation and sulfate pulse. Soil Biology and Biochemistry, **35**, 535-547.
 - Borge AF, Westermann S, Solheim I, Etzelmüller B (2017) Strong degradation of palsas and peat plateaus in northern Norway during the last 60 years. The Cryosphere, **11**, 1-16.
 - Bridgham SD, Cadillo- Quiroz H, Keller JK, Zhuang Q (2013) Methane emissions from wetlands: biogeochemical, microbial, and modeling perspectives from local to global scales. Global Change Biology, 19, 1325-1346.
 - Brookes PC, Landman A, Pruden G, Jenkinson DS (1985) Chloroform fumigation and the release of soil nitrogen: a rapid direct extraction method to measure microbial biomass nitrogen in soil. Soil Biology and Biochemistry, **17**, 837-842.
 - Burke EJ, Ekici A, Huang Y *et al.* (2017) Quantifying uncertainties of permafrost carbonclimate feedbacks. Biogeosciences, **14**, 3051.
 - Christensen TR, Jackowicz-Korczyński M, Aurela M, Crill P, Heliasz M, Mastepanov M, Friborg T (2012) Monitoring the multi-year carbon balance of a subarctic palsa mire with micrometeorological techniques. Ambio, 41, 207-217.
 - Christensen TR, Johansson T, Åkerman HJ *et al.* (2004) Thawing sub- arctic permafrost: Effects on vegetation and methane emissions. Geophysical Research Letters, **31**, L04501.
 - Christensen TR, Jonasson S, Callaghan TV, Havstrom M (1999) On the potential CO₂ release from tundra soils in a changing climate. Applied Soil Ecology, **11**, 127-134.
 - Christiansen JR, Romero AJB, Jørgensen NOG, Glaring MA, Jørgensen CJ, Berg LK, Elberling B (2015) Methane fluxes and the functional groups of methanotrophs and

methanogens in a young Arctic landscape on Disko Island, West Greenland. Biogeochemistry, **122**, 15-33.

- Ciais P, Sabine C, Bala G et al. (2013) Carbon and other biogeochemical cycles. In: Climate change 2013: the physical science basis. Contribution of Working Group I to the Fifth Assessment Report of the Intergovernmental Panel on Climate Change. (eds Stocker TF, Qin D, Plattner GK, Tignor M, Allen SK, Boschung J, Nauels A, Xia Y, Bex V, Midgley PM), pp 465-570, Cambridge, United Kingdom and New York, NY, USA, Cambridge University Press.
- Cooper MD, Estop-Aragonés C, Fisher JP *et al.* (2017) Limited contribution of permafrost carbon to methane release from thawing peatlands. Nature Climate Change, **7**, 507-513.
- Corbett JE, Burdige DJ, Tfaily MM, Dial AR, Cooper WT, Glaser PH, Chanton JP (2013) Surface production fuels deep heterotrophic respiration in northern peatlands. Global Biogeochemical Cycles, **27**, 1163-1174.
- D'imperio L, Nielsen CS, Westergaard- Nielsen A, Michelsen A, Elberling B (2017)
 Methane oxidation in contrasting soil types: responses to experimental warming with implication for landscape- integrated CH4 budget. Global Change Biology, 23, 966-976.
- Deng J, Li C, Frolking S, Zhang Y, Backstrand K, Crill P (2014) Assessing effects of permafrost thaw on C fluxes based on multiyear modeling across a permafrost thaw gradient at Stordalen, Sweden. Biogeosciences, **11**, 4753-4770.
- Diakova K, Capek P, Kohoutova I *et al.* (2016) Heterogeneity of carbon loss and its temperature sensitivity in East-European subarctic tundra soils. FEMS microbiology ecology, **92**, 1-17.

- Dorodnikov M, Marushchak M, Biasi C, Wilmking M (2013) Effect of microtopography on isotopic composition of methane in porewater and efflux at a boreal peatland. Boreal Environment Research, **18**, 269–279.
- Dorrepaal E, Toet S, Van Logtestijn RSP, Swart E, Van De Weg MJ, Callaghan TV, Aerts R (2009) Carbon respiration from subsurface peat accelerated by climate warming in the subarctic. Nature, **460**, 616-620.
- Estop-Aragonés C, Cooper MDA, Fisher JP *et al.* (2018a) Limited release of previouslyfrozen C and increased new peat formation after thaw in permafrost peatlands. Soil Biology and Biochemistry, **118**, 115-129.
- Estop-Aragonés C, Czimczik CI, Heffernan L, Gibson C, Walker JC, Xu X, Olefeldt D (2018b) Respiration of aged soil carbon during fall in permafrost peatlands enhanced by active layer deepening following wildfire but limited following thermokarst. Environmental Research Letters, **13**, 085002.
- Euskirchen ES, Edgar CW, Turetsky MR, Waldrop MP, Harden JW (2014) Differential response of carbon fluxes to climate in three peatland ecosystems that vary in the presence and stability of permafrost. Journal of Geophysical Research: Biogeosciences, **119**, 1576-1595.
- Flessa H, Rodionov A, Guggenberger G *et al.* (2008) Landscape controls of CH4 fluxes in a catchment of the forest tundra ecotone in northern Siberia. Global Change Biology, 14, 2040-2056.
- Frolking S, Roulet NT (2007) Holocene radiative forcing impact of northern peatland carbon accumulation and methane emissions. Global Change Biology, **13**, 1079-1088.
- Gorham E (1991) Northern peatlands: Role in the carbon cycle and probable responses to climatic warming. Ecological Applications, **1**, 182-195.

- Grogan P, Chapin FS (2000) Initial effects of experimental warming on above-and belowground components of net ecosystem CO₂ exchange in arctic tundra. Oecologia, 125, 512-520.
- Hayes DJ, Kicklighter DW, Mcguire AD *et al.* (2014) The impacts of recent permafrost thaw on land-atmosphere greenhouse gas exchange. Environmental Research Letters, **9**, 045005.
- Haynes K, Connon R, Quinton WJERL (2018) Permafrost thaw induced drying of wetlands at Scotty Creek, NWT, Canada. Environmental Research Letters, **13**, 114001.
- Heikkinen JEP, Elsakov V, Martikainen PJ (2002) Carbon dioxide and methane dynamics and annual carbon balance in tundra wetland in NE Europe, Russia. Global Biogeochemical Cycles, **16**, 62-61-62-15.
- Helbig M, Chasmer LE, Desai AR, Kljun N, Quinton WL, Sonnentag O (2017a) Direct and indirect climate change effects on carbon dioxide fluxes in a thawing boreal forest– wetland landscape. Global Change Biology, 23, 3231-3248.
- Helbig M, Chasmer LE, Kljun N, Quinton WL, Treat CC, Sonnentag O (2017b) The positive net radiative greenhouse gas forcing of increasing methane emissions from a thawing boreal forest- wetland landscape. Global Change Biology, 23, 2413-2427.
- Hicks Pries CE, Logtestijn RSP, Schuur EaG, Natali SM, Cornelissen JHC, Aerts R, Dorrepaal E (2015) Decadal warming causes a consistent and persistent shift from heterotrophic to autotrophic respiration in contrasting permafrost ecosystems. Global Change Biology, 21, 4508-4519.
- Hobbie SE, Miley TA, Weiss MS (2002) Carbon and nitrogen cycling in soils from acidic and nonacidic tundra with different glacial histories in Northern Alaska. Ecosystems, 5, 761-774.

- Hodgkins SB, Tfaily MM, Mccalley CK *et al.* (2014) Changes in peat chemistry associated with permafrost thaw increase greenhouse gas production. Proceedings of the National Academy of Sciences of the United States of America, **111**, 5819-5824.
- Hugelius G, Routh J, Kuhry P, Crill P (2012) Mapping the degree of decomposition and thaw remobilization potential of soil organic matter in discontinuous permafrost terrain.Journal of Geophysical Research: Biogeosciences, **117**, G02030-G02030.
- Hugelius G, Strauss J, Zubrzycki S *et al.* (2014) Estimated stocks of circumpolar permafrost carbon with quantified uncertainty ranges and identified data gaps. Biogeosciences, 11, 6573-6593.
- Hugelius G, Virtanen T, Kaverin D *et al.* (2011) High-resolution mapping of ecosystem carbon storage and potential effects of permafrost thaw in periglacial terrain, European Russian Arctic. Journal of Geophysical Research: Biogeosciences, 116, G03024-G03024.
- Johnston CE, Ewing SA, Harden JW *et al.* (2014) Effect of permafrost thaw on CO₂ and CH₄ exchange in a western Alaska peatland chronosequence. Environmental Research Letters, **9**, 085004.
- Jones MC, Harden J, O'donnell J, Manies K, Jorgenson T, Treat C, Ewing S (2017) Rapid carbon loss and slow recovery following permafrost thaw in boreal peatlands. Global Change Biology, **23**, 1109-1127.
- Jørgensen CJ, Johansen KML, Westergaard-Nielsen A, Elberling B (2015) Net regional methane sink in High Arctic soils of northeast Greenland. Nature Geoscience, **8**, 20-23.
- Knoblauch C, Beer C, Liebner S, Grigoriev MN, Pfeiffer E-M (2018) Methane production as key to the greenhouse gas budget of thawing permafrost. Nature Climate Change, 8, 309-312.

- Knoblauch C, Beer C, Sosnin A, Wagner D, Pfeiffer EM (2013) Predicting long- term carbon mineralization and trace gas production from thawing permafrost of Northeast Siberia. Global Change Biology, **19**, 1160-1172.
- Knorr K-H, Blodau C (2009) Impact of experimental drought and rewetting on redox transformations and methanogenesis in mesocosms of a northern fen soil. Soil Biology and Biochemistry, 41, 1187-1198.
- Komulainen V-M, Nykänen H, Martikainen PJ, Laine J (1998) Short-term effect of restoration on vegetation change and methane emissions from peatlands drained for forestry in southern Finland. Canadian Journal of Forest Research, **28**, 402-411.
- Koven CD, Ringeval B, Friedlingstein P *et al.* (2011) Permafrost carbon-climate feedbacks accelerate global warming. **108**, 14769-14774.
- Koven CD, Schuur EA, Schadel C *et al.* (2015) A simplified, data-constrained approach to estimate the permafrost carbon-climate feedback. Philosophical transactions.Series A, Mathematical, physical, and engineering sciences, **373**, 20140423.
- Kuhry P (2008) Palsa and peat plateau development in the Hudson Bay Lowlands, Canada: timing, pathways and causes. Boreas, 37, 316-327.
- Kuzyakov Y (2010) Priming effects: interactions between living and dead organic matter.Soil Biology and Biochemistry, 42, 1363-1371.
- Lafleur PM, Humphreys ER, St. Louis VL *et al.* (2012) Variation in peak growing season net ecosystem production across the Canadian Arctic. Environmental science & technology, **46**, 7971-7977.

Lai DYF (2009) Methane Dynamics in Northern Peatlands: A Review. Pedosphere, **19**, 409-421.

- Lara MJ, Genet H, Mcguire AD *et al.* (2016) Thermokarst rates intensify due to climate change and forest fragmentation in an Alaskan boreal forest lowland. Global Change Biology, **22**, 816-829.
- Lau MC, Stackhouse BT, Layton AC *et al.* (2015) An active atmospheric methane sink in high Arctic mineral cryosols. The ISME journal, **9**, 1880-1891.
- Lee H, Schuur EaG, Inglett KS, Lavoie M, Chanton JP (2012) The rate of permafrost carbon release under aerobic and anaerobic conditions and its potential effects on climate. Global Change Biology, 18, 515-527.
- Lide DR, Frederikse HPR (1995) CRC handbook of chemistry and physics, Vol. 76, Boca Raton, CRC Press, USA.
- Liljedahl AK, Boike J, Daanen RP *et al.* (2016) Pan-Arctic ice-wedge degradation in warming permafrost and its influence on tundra hydrology. Nature Geoscience, **9**, 312-319.
- Lund M, Falk JM, Friborg T, Mbufong HN, Sigsgaard C, Soegaard H, Tamstorf MP (2012) Trends in CO₂ exchange in a high Arctic tundra heath, 2000–2010. Journal of Geophysical Research: Biogeosciences, **117**, G02001.
- Lundin EJ, Klaminder J, Giesler R *et al.* (2016) Is the subarctic landscape still a carbon sink?
 Evidence from a detailed catchment balance. Geophysical Research Letters, 43, 1988-1995.
- Malhotra A, Roulet NT (2015) Environmental correlates of peatland carbon fluxes in a thawing landscape: do transitional thaw stages matter? Biogeosciences, 12, 3119-3130.
- Malmer N, Johansson T, Olsrud M, Christensen TR (2005) Vegetation, climatic changes and net carbon sequestration in a North- Scandinavian subarctic mire over 30 years. Global Change Biology, 11, 1895-1909.

- Marushchak ME, Pitkamaki A, Koponen H, Biasi C, Seppala M, Martikainen PJ (2011) Hot spots for nitrous oxide emissions found in different types of permafrost peatlands.Global Change Biology, 17, 2601-2614.
- Mastepanov M, Christensen TR (2009) Laboratory investigations of methane buildup in, and release from, shallow peats. Carbon Cycling in Northern Peatlands, **184**, 205-218.
- Mauritz M, Bracho R, Celis G *et al.* (2017) Nonlinear CO₂ flux response to 7 years of experimentally induced permafrost thaw. Global Change Biology, **23**, 3646-3666.
- Mccalley CK, Woodcroft BJ, Hodgkins SB *et al.* (2014) Methane dynamics regulated by microbial community response to permafrost thaw. Nature, **514**, 478-484.
- Mcguire AD, Lawrence DM, Koven C *et al.* (2018) Dependence of the evolution of carbon dynamics in the northern permafrost region on the trajectory of climate change.
 Proceedings of the National Academy of Sciences of the United States of America, 115, 3882-3887.
- Moore TR, Knowles R (1989) The influence of water table levels on methane and carbon dioxide emissions from peatland soils. Canadian Journal of Soil Science, **69**, 33-38.
- Myhre G, Shindell D, Bréon F-M *et al.* (2013) Anthropogenic and natural radiative forcing.
 In: *Climate Change 2013: The Physical Science Basis. Contribution of Working Group I to the Fifth Assessment Report of the Intergovernmental Panel on Climate Change.* (eds Stocker TF, Qin D, Plattner GK, Tignor M, Allen SK, Boschung J,
 Nauels A, Xia Y, Bex V, Midgley PM), pp 659-740, Cambridge, United Kingdom
 and New York, NY, USA, Cambridge University Press.
- Neubauer SC, Givler K, Valentine S, Megonigal JPJE (2005) Seasonal patterns and plant- mediated controls of subsurface wetland biogeochemistry. Ecology, **86**, 3334-3344.

- Neubauer SC, Megonigal JP (2015) Moving Beyond Global Warming Potentials to Quantify the Climatic Role of Ecosystems. Ecosystems, **18**, 1000-1013.
- Nykänen H, Heikkinen JEP, Pirinen L, Tiilikainen K, Martikainen PJ (2003) Annual CO₂ exchange and CH₄ fluxes on a subarctic palsa mire during climatically different years. Global Biogeochemical Cycles, **17**, 1-18.
- O'donnell JA, Jorgenson MT, Harden JW, Mcguire AD, Kanevskiy MZ, Wickland KP (2012) The effects of permafrost thaw on soil hydrologic, thermal, and carbon dynamics in an Alaskan peatland. Ecosystems, **15**, 213-229.
- Oechel WC, Hastings SJ, Vourlitis G, Jenkins M, Riechers G, Grulke N (1993) Recent change of Arctic tundra ecosystems from a net carbon dioxide sink to a source. Nature, **361**, 520-523.
- Olefeldt D, Goswami S, Grosse G *et al.* (2016) Circumpolar distribution and carbon storage of thermokarst landscapes. Nature Communications, **7**, 13043.
- Olefeldt D, Roulet NT (2012) Effects of permafrost and hydrology on the composition and transport of dissolved organic carbon in a subarctic peatland complex. Journal of Geophysical Research: Biogeosciences, **117**, G01005.
- Olefeldt D, Turetsky MR, Crill PM, Mcguire AD (2013) Environmental and physical controls on northern terrestrial methane emissions across permafrost zones. Global Change Biology, **19**, 589-603.
- Palonen V, Oinonen M (2013) Molecular sieves in 14CO2 sampling and handling. Radiocarbon, **55**, 416-420.
- Palonen V, Pesonen A, Herranen T, Tikkanen P, Oinonen M (2013) HASE–The Helsinki adaptive sample preparation line. Nuclear Instruments and Methods in Physics
 Research Section B: Beam Interactions with Materials and Atoms, 294, 182-184.

R Core Team (2018) R: A language and environment for statistical computing.

- Regina K, Silvola J, Martikainen PJ (1999) Short- term effects of changing water table on N₂O fluxes from peat monoliths from natural and drained boreal peatlands. Global Change Biology, 5, 183-189.
- Repo ME, Susiluoto S, Lind SE *et al.* (2009) Large N₂O emissions from cryoturbated peat soil in tundra. Nature Geoscience, **2**, 189-192.
- Romanovsky VE, Drozdov DS, Oberman NG *et al.* (2010) Thermal State of Permafrost in Russia. Permafrost and Periglacial Processes, **21**, 136-155.
- Salmon VG, Soucy P, Mauritz M, Celis G, Natali SM, Mack MC, Schuur EaG (2016) Nitrogen availability increases in a tundra ecosystem during five years of experimental permafrost thaw. Global Change Biology, **22**, 1927-1941.
- Sannel ABK, Kuhry P (2011) Warming- induced destabilization of peat plateau/thermokarst lake complexes. Journal of Geophysical Research: Biogeosciences, **116**, G03035.
- Saunois M, Bousquet P, Poulter B *et al.* (2016) The global methane budget 2000-2012. Earth System Science Data, **8**, 697-751.
- Schädel C, Bader MKF, Schuur EaG *et al.* (2016) Potential carbon emissions dominated by carbon dioxide from thawed permafrost soils. Nature Climate Change, **6**, 950-953.
- Schädel C, Koven CD, Lawrence DM *et al.* (2018) Divergent patterns of experimental and model-derived permafrost ecosystem carbon dynamics in response to Arctic warming.
 13, 105002.
- Schädel C, Luo Y, Evans RD, Fei S, Schaeffer SMJO (2013) Separating soil CO₂ efflux into C-pool-specific decay rates via inverse analysis of soil incubation data. Oecologia, 171, 721-732.
- Schaefer K, Lantuit H, Romanovsky VE, Schuur EaG, Witt R (2014) The impact of the permafrost carbon feedback on global climate. Environmental Research Letters, **9**, 085003.

- Schuur EaG, Abbott BW, Bowden WB *et al.* (2013) Expert assessment of vulnerability of permafrost carbon to climate change. Climatic Change, **119**, 359-374.
- Schuur EaG, Bockheim J, Canadell JG *et al.* (2008) Vulnerability of permafrost carbon to climate change: Implications for the global carbon cycle. Bioscience, **58**, 701-714.
- Schuur EaG, Mcguire AD, Schaedel C *et al.* (2015) Climate change and the permafrost carbon feedback. Nature, **520**, 171-179.
- Schuur EaG, Vogel JG, Crummer KG, Lee H, Sickman JO, Osterkamp TE (2009) The effect of permafrost thaw on old carbon release and net carbon exchange from tundra. Nature, **459**, 556-559.
- Seppälä M (2003) Surface abrasion of palsas by wind action in Finnish Lapland. Geomorphology, **52**, 141-148.

Seppälä M (2006) Palsa mires in Finland. The Finnish environment, 23, 155-162.

Shaver GR, Street LE, Rastetter EB, Van Wijk MT, Williams M (2007) Functional convergence in regulation of net CO2 flux in heterogeneous tundra landscapes in Alaska and Sweden. Journal of Ecology, 95, 802-817.

Stuiver M, Polach HA (1977) Discussion reporting of 14 C data. Radiocarbon, 19, 355-363.

- Sturtevant CS, Oechel WC (2013) Spatial variation in landscape- level CO₂ and CH₄ fluxes from arctic coastal tundra: influence from vegetation, wetness, and the thaw lake cycle. Global Change Biology, **19**, 2853-2866.
- Swindles GT, Morris PJ, Mullan D *et al.* (2015) The long-term fate of permafrost peatlands under rapid climate warming. Scientific reports, **5**, 17951.

- Tarnocai C, Canadell JG, Schuur EaG, Kuhry P, Mazhitova G, Zimov S (2009) Soil organic carbon pools in the northern circumpolar permafrost region. Global Biogeochemical Cycles, 23, GB2023.
- Tikkanen P, Palonen V, Jungner H, Keinonen J (2004) AMS facility at the University of Helsinki. Nuclear Instruments and Methods in Physics Research Section B: Beam Interactions with Materials and Atoms, 223, 35-39.
- Treat CC, Bloom AA, Marushchak ME (2018) Nongrowing season methane emissions-a significant component of annual emissions across northern ecosystems. Global Change Biology, 24, 3331-3343.
- Treat CC, Jones MC, Camill P *et al.* (2016) Effects of permafrost aggradation on peat properties as determined from a pan- Arctic synthesis of plant macrofossils. Journal of Geophysical Research: Biogeosciences, **121**, 78-94.
- Treat CC, Natali SM, Ernakovich J *et al.* (2015) A pan- Arctic synthesis of CH₄ and CO₂ production from anoxic soil incubations. Global Change Biology, **21**, 2787-2803.
- Treat CC, Wollheim WM, Varner RK, Grandy AS, Talbot J, Frolking S (2014) Temperature and peat type control CO₂ and CH₄ production in Alaskan permafrost peats. Global Change Biology, **20**, 2674-2686.
- Tuittila E-S, Komulainen V-M, Vasander H, Laine J (1999) Restored cut-away peatland as a sink for atmospheric CO₂. Oecologia, **120**, 563-574.
- Turetsky MR, Wieder RK, Vitt DH (2002) Boreal peatland C fluxes under varying permafrost regimes. Soil Biology & Biochemistry, **34**, 907-912.
- Vance ED, Brookes PC, Jenkinson DS (1987) An extraction method for measuring soil microbial biomass C. Soil Biology and Biochemistry, **19**, 703-707.

- Voigt C, Lamprecht RE, Marushchak ME *et al.* (2017a) Warming of subarctic tundra increases emissions of all three important greenhouse gases carbon dioxide, methane, and nitrous oxide. Glob Chang Biol, **23**, 3121-3138.
- Voigt C, Marushchak ME, Lamprecht RE *et al.* (2017b) Increased nitrous oxide emissions from Arctic peatlands after permafrost thaw. Proceedings of the National Academy of Sciences of the United States of America, **114**, 6238-6243.
- Vonk JE, Gustafsson Ö (2013) Permafrost-carbon complexities. Nature Geoscience, **6**, 675-676.
- Walz J, Knoblauch C, Böhme L, Pfeiffer E-M (2017) Regulation of soil organic matter decomposition in permafrost-affected Siberian tundra soils-Impact of oxygen availability, freezing and thawing, temperature, and labile organic matter. Soil Biology and Biochemistry, **110**, 34-43.
- Wang Z, Roulet N (2017) Comparison of plant litter and peat decomposition changes with permafrost thaw in a subarctic peatland. Plant and Soil, **417**, 197-216.
- Wild B, Gentsch N, Capek P *et al.* (2016) Plant-derived compounds stimulate the decomposition of organic matter in arctic permafrost soils. Scientific reports, 6, 25607.
- Wild B, Schnecker J, Alves RJE *et al.* (2014) Input of easily available organic C and N stimulates microbial decomposition of soil organic matter in arctic permafrost soil. Soil Biology and Biochemistry, **75**, 143-151.
- Wilson RM, Fitzhugh L, Whiting GJ *et al.* (2017) Greenhouse gas balance over thaw- freeze cycles in discontinuous zone permafrost. Journal of Geophysical Research: Biogeosciences, **122**, 387-404.
- Zamolodchikov D, Karelin D, Ivaschenko A (2000) Sensitivity of tundra carbon balance to ambient temperature. Water, air, and soil pollution, **119**, 157-169.

Fig. 1: Carbon dioxide (CO₂) (a) and methane (CH₄) fluxes (b) from the four treatments (mean±SE, n = 4): DB = dry bare, WB = wet bare, DV = dry vegetated, WV = wet vegetated. Seasonal thaw = thawing of the active layer (0–65cm), permafrost = thawing of permafrost (65–80cm). To exclude the effect of a temporarily lowered water table level, CO₂ and CH₄ flux values in the wet mesocosms were discarded for the three days following initiation of each thawing stage, and when the water table dropped below 10cm during the experiment. Measured (hourly) flux rates (light green line) are shown with data gaps, whereas daily mean flux rates (dark green line) for these time

periods were interpolated linearly. The time series including periods with water table fluctuations are shown in Fig. S3. Thawing steps, week 1: Thawing down to ~20 cm, week 5: thawing down to ~40 cm, week 9: thawing down to 5 cm above the maximum seasonal thaw depth; week 13: thawing down to the maximum seasonal thaw depth; week 17: thawing down to 5 cm below the maximum seasonal thaw depth; week 21: thawing of the full core (15 cm below the maximum seasonal thaw depth). Flux rates of individual replicates are provided as Supporting Information (Fig. S4–S7).

Fig. 2: Mean daily fluxes of CO_2 and CH_4 for the four-week period before thawing the permafrost (week 13–16, thawing of the whole active layer) and the four week period after thawing the deeper permafrost (week 21–24, thawing of the whole core). Note deviating scaling of y-axis for CO_2 and CH_4 . Flux peaks related to a thawing-induced, temporarily lowered water table in the wet mesocosms were removed from the analysis; see Table S3 for details. Data are shown for bare and vegetated mesocosms with natural ("dry") and artificially raised (5–10 cm below surface, "wet")

water table, referred to as DB = dry bare, DV = dry vegetated, WB = wet bare, WV = wet vegetated. Boxplots show mean (thick black line), median (dotted black line), upper and lower quartile, as well as the smallest and largest value. n = 4 for all treatments except for DV post-thaw (n = 2). Levels of significance: ***significant at $P \le 0.001$, **significant at $P \le 0.01$, *significant at $P \le 0.05$.

Fig. 3: Cumulative carbon dioxide (CO₂) and methane (CH₄) fluxes, calculated as CO₂–eq during each thawing step (lasting four weeks each). Seasonal thaw = thawing of the active layer (0–65cm), permafrost = thawing of permafrost (65–80cm). Data are shown for bare and vegetated mesocosms with natural ("dry") and artificially raised (5–10 cm below surface, "wet") water table, referred to as DB = dry bare, DV = dry vegetated, WB = wet bare, WV = wet vegetated. Boxplots show median (thick black line), upper and lower quartile, as well as the smallest and largest value. n = 4 unless otherwise specified. Arrows used to emphasize increasing trend in CO₂ emissions when thawing the permafrost layer. Inset in DB: Radiocarbon (¹⁴C) age of C respired. Thick black line in boxplots for ¹⁴C age represents mean, dotted black line is the median.

Fig. 4: Soil profile concentrations of gaseous and dissolved carbon dioxide (CO₂), methane (CH₄) and dissolved organic carbon (DOC) in mesocosms for the duration of the experiment. Seasonal thaw = thawing of the active layer (0–65cm), permafrost = thawing of permafrost (65–80cm). Data are shown for bare and vegetated mesocosms with natural ("dry") and artificially raised (5–10 cm below surface, "wet") water table, referred to as DB = dry bare, DV = dry vegetated, WB = wet bare, WV = wet vegetated. Contour plots were created by linear interpolation between measurement points. For CO₂ and CH₄ the number of measurement points per mesocosm was 26 and for DOC the figure includes 15 measurement points. White areas: no data available due to frozen soil conditions. Thick red line indicates thaw depths over time, dashed lines indicate thawing steps, and thick grey line

marks a zone of below ambient CH_4 concentration. Thawing steps, week 1: Thawing down to ~20 cm, week 5: thawing down to ~40 cm, week 9: thawing down to 5 cm above the maximum seasonal thaw depth; week 13: thawing down to the maximum seasonal thaw depth; week 17: thawing down to 5 cm below the maximum seasonal thaw depth; week 21: thawing of the full core (15 cm below the maximum seasonal thaw depth). Note logarithmic scaling of colour scale for CH_4 . Gas concentrations of individual replicates are provided as Supporting Information (Fig. S8-S11).

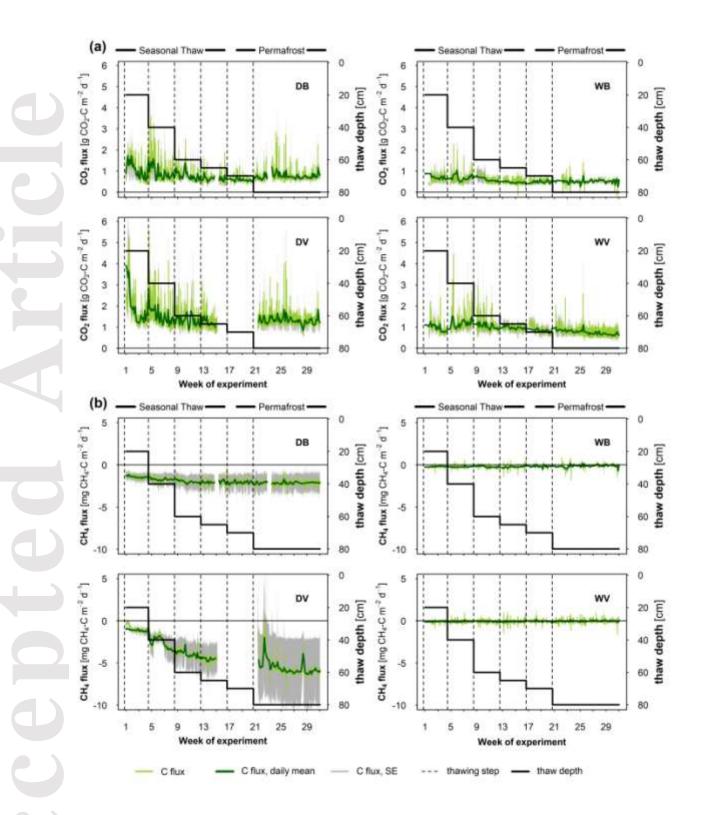
Fig. 5: Cumulative fluxes of carbon dioxide (CO₂), methane (CH₄), nitrous oxide (N₂O), and total greenhouse gas (GHG) emissions expressed as (a) global warming potential (GWP) and (b) sustained-flux global warming/cooling potentials (SGWP/SGCP) from the four treatments mean±SE, n = 4): DB = dry bare, WB = wet bare, DV = dry vegetated, WV = wet vegetated. Seasonal thaw = thawing of the active layer (0–65cm), permafrost = thawing of permafrost (65–80cm). The cumulative sum of total GHG emissions (dashed black line) and of CO₂ (light blue line) are indicated on the y-axis. Grey areas show uncertainty (SE) of CO₂, CH₄ and N₂O fluxes. Data for N₂O fluxes are taken from Voigt *et al.*, 2017. Conversion factors for (a) CH₄: 28, N₂O: 265, (b) CH₄ emissions: 45, CH₄ uptake: 203, N₂O emissions: 270, N₂O uptake: 349. Thawing steps, week 1: Thawing down to ~20 cm, week 5: thawing down to ~40 cm, week 9: thawing down to 5 cm above the maximum seasonal thaw depth; week 13: thawing down to 5 cm below the maximum seasonal thaw depth; week 21: thawing of the full core (15 cm below the maximum seasonal thaw depth).

Fig. 6: Mean measured flux rates of carbon dioxide (CO₂) and methane (CH₄) from bare and vegetated mesocosms (weeks 1–16, thawing of the active layer) and *in situ* measurements at the sampling site ("Peera Palsa" near Kilpisjärvi, 68.88°N, 21.05°E), as well as published, *in situ* flux rates

from a range of permafrost peatlands in northern Finland (palsa mires) (Marushchak *et al.*, 2011, Nykänen *et al.*, 2003) and western Russia (peat plateau) (Voigt *et al.*, 2017a). Spring: June, summer: July and August, autumn: September, n. d.= not determined. Boxplots show median (thick black line), upper and lower quartile, as well as the smallest and largest value.

Table 1: Permafrost contribution to carbon dioxide (CO₂) flux in the weeks following permafrost thaw for each experimental treatment. Flux peaks related to a thawing-induced, temporarily lowered water table in the wet mesocosms were removed from the analysis; see Table S3 for details. Flux values are shown as mean±SD for the four-week period after thawing the permafrost part of the mesocosms (week 21–24); further time periods are presented in Table S10.

Treatment	$\Delta_{measured - predicted}$	Permafrost
	$(g CO_2 - C m^{-2} d^{-1})$	contribution
dry bare (DB)	0.20 ± 0.17	22 %
dry vegetated (DV)	0.16 ± 0.22	10 %
wet bare (WB)	0.02 ± 0.08	4 %
wet vegetated (WV)	-0.01 ± 0.01	-2 %



This article is protected by copyright. All rights reserved.

